

Analysis of Noise for Rapid-Scan and Step-Scan Methods of FT-IR Difference Spectroscopy

STEVEN S. ANDREWS* and STEVEN G. BOXER

Department of Chemistry, Stanford University, Stanford, California 94305-5080

Quantitative vibrational difference spectroscopy of small signals requires techniques that minimize spectral noise. As simple modulation of the sample followed by signal demodulation is often problematic due to interference with the FT-IR Fourier frequencies, alternate methods are necessary. Using vibrational Stark spectroscopy as an example, the DC method involves alternating complete interferogram scans in which a DC electric field is turned on with scans in which the field is turned off. A new synchronized AC method is similar, but the field is switched at every interferogram sampling point. In the step-scan method, a sinusoidal electric field is used and the detector signal is demodulated with a lock-in amplifier at each mirror position. Noise levels for these methods are derived analytically in this paper and compared with experimental values, yielding results that are broadly applicable to FT-IR difference spectroscopy. It was found that the DC method performed the best, although specific experimental factors may favor other methods.

Index Headings: Step-scan FT-IR; Rapid-scan FT-IR; Vibrational Stark; Noise analysis.

INTRODUCTION

While infrared spectroscopy has historically been used most often as a qualitative tool, it is rapidly gaining utility as a precision technique. The example used throughout this paper is that of vibrational Stark effect spectroscopy,¹ where a Stark spectrum is the infrared spectrum of a sample in the presence of an external electric field minus the spectrum of the sample without the field. Stark spectra are useful both as a means to probe electric-field changes in locally structured systems² and as a way of studying the physics of molecular vibrations.^{3,4} Other infrared difference methods include vibrational linear⁵ and circular⁶ dichroism, reflection-absorption measurements of adsorbed films,⁷ difference spectra of electrochemically modulated species,^{8,9} and time-resolved infrared spectroscopy.¹⁰⁻¹³

Difference spectra for these techniques, as well as many others, involve very small signals. Using the vibrational Stark example, if a sample of acetonitrile has a peak absorption of 0.2 o.d. (optical density unit) in the absence of an applied field, then the peak will decrease by 5×10^{-4} o.d. in a 1 MV/cm applied field.¹ The difference is much smaller away from the absorption maximum, but these spectral regions are still essential for data analysis, so it is necessary to achieve noise levels well below 5×10^{-5} o.d. This example involves a fairly ideal sample; a sample concentration that gives 0.2 o.d. is often not achievable, electric breakdown of samples generally occurs below 1 MV/cm, and many interesting samples have smaller Stark effects, all of which lead to smaller signals and require even lower noise.

The standard method of Stark spectroscopy with dispersive instruments involves electric-field modulation at about 200 Hz, followed by detector signal demodulation using a lock-in amplifier.¹⁴ This method cannot be directly applied to continuous-scan FT-IR measurements since the sample modulation frequency needs to be much faster or much slower than the Fourier frequencies to avoid signal interference effects. Fourier frequencies from the interferometer range from 100 Hz to 10 kHz for typical scan speeds and for mid-infrared measurements, while electric fields can be modulated only up to between 2 and 3 kHz due to the capacitance and resistance of the sample cells currently in use. The frequency separation can be achieved by stopping the field, by stopping the Fourier frequencies, or by keeping the field and the mirror synchronized, methods which are shown in Fig. 1 and explained below. Dichroism measurements typically modulate the light polarization at about 50 kHz, permitting other methods, which are described below as well.

In DC Stark spectroscopy,¹ a complete interferogram is measured in rapid-scan mode with a DC electric field turned on, followed by a scan with the field turned off. This cycle is repeated several hundred times for signal averaging, while separately co-adding field-on and field-off interferograms. The interferograms are Fourier transformed to yield single channel spectra, and the negative log of their ratio gives the Stark effect difference spectrum. For synchronized AC measurements, a method that has not been reported before, the electric field is switched rapidly, such that it is turned on for only the even numbered interferogram points of one scan and only the odd numbered points of the next scan. After co-adding many repetitions, the field-on points are collected into one interferogram and the field-off points are collected into a different interferogram; the interferograms are analyzed as for the DC method. For the step-scan method, the moving mirror is stopped and then stepped sequentially to each of the sample positions.^{15,16} At each retardation, the electric field is modulated sinusoidally and a lock-in amplifier measures the detector output at twice the field frequency (which is the frequency with maximum sample response since the response is proportional to the square of the field). The output signal from the lock-in comprises a difference interferogram, which is Fourier transformed and divided by the total light intensity through the sample (measured separately) to yield a Stark effect difference spectrum. For situations in which the sample modulation is too slow for high detectivity, phase modulation, in which the moving mirror is rapidly dithered during a step-scan measurement,¹⁵ can be used to provide a high-frequency carrier signal.

It is not immediately obvious which difference spec-

Received 29 January 2001; accepted 4 May 2001.

* Author to whom correspondence should be sent.

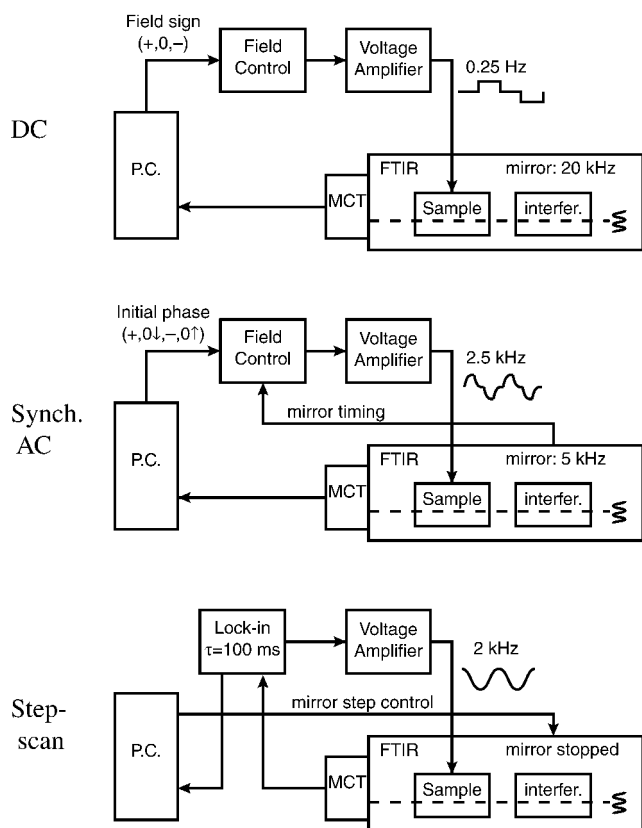


FIG. 1. Schematic diagram of vibrational Stark spectroscopy methods. The P.C. box represents both a computer and some FT-IR electronics. In the synchronized AC diagram, the $0\uparrow$ and $0\downarrow$ symbols represent starting states with the field off, followed by a positive or negative field at the next point, respectively.

troscopy method should give the best signal-to-noise ratio. This paper presents calculations of the noise levels for the three methods as well as experimentally measured noise levels. The calculations are useful because they show how various experimental parameters affect signal-to-noise ratios, which greatly simplifies the optimization of experiments and also shows what experiments are feasible. While this paper focuses on measurements of the vibrational Stark effect, results are broadly applicable to other types of infrared difference spectroscopy.

Other types of FT-IR difference spectroscopy are available for dichroism measurements or other techniques that allow fast sample modulation. For double modulation,^{17,18} the sample is modulated at high frequency while the interferometer is in rapid-scan mode, using a slow mirror speed. The detector is demodulated with a lock-in amplifier set to the sample modulation frequency to yield a difference interferogram, which is analyzed as for the step-scan method. Signal-to-noise ratios for double modulation in the mid-infrared region have been shown to be similar to those for the step-scan method.¹⁹ For frequencies above 2000 cm^{-1} , double modulation is progressively more difficult since shorter lock-in time constants are required to pass the higher Fourier frequencies.¹⁶ An adaptation of the double modulation method has been presented⁷ in which the signal is demodulated not with a lock-in amplifier, but synchronously with the sample modulation using video sample-and-hold amplifiers and summing amplifiers. This allows the use of a faster mirror

speed and eliminates some artifacts associated with double modulation. A wide variety of methods for time-resolved spectroscopy have been presented as well,^{10,12,20–23} several of which are conceptually analogous to ones presented above.

EXPERIMENTAL

Spectra were measured with a Bruker IFS 66V/S FT-IR with an externally mounted EG&G narrow band MCT detector (model J15D14-M204B-S01M). The detector has a 1 mm^2 detector element and a D^* value of $3.4 \times 10^{10}\text{ cm}(\text{Hz})^{1/2}\text{ W}^{-1}$. To prevent detector saturation, light was limited with a 2-mm-diameter aperture and with a room-temperature variable interference filter positioned to transmit light between 1400 and 2330 cm^{-1} placed between the sample and the detector. The Stark effect setup is described elsewhere.¹ The sample was a dilute solution of methyl-vinyl-ketone dissolved in 2-methyl-tetrahydrofuran, and frozen to create a uniform isotropic glass. The carbonyl stretch mode of methyl-vinyl-ketone has a Stark difference dipole of 0.049 D/f , yielding a Stark effect between those found for many nitriles¹ and those for carbon monoxide bound to heme proteins.² In terms of the detector response, light intensity through the sample was 7.4 mV/cm^{-1} at 1750 cm^{-1} . Applied electric fields were 0.50 MV/cm for the DC method and synchronized AC method and 0.36 rms MV/cm for step-scan (peak field of 0.50 MV/cm). To maximize uniformity, all spectra presented were measured with 40 min of signal averaging, 1 cm^{-1} resolution, single-sided data acquisition, using the same sample, and during the same day. Fourier transforms used a zero-filling factor of 2, Mertz phase correction (signed Mertz with stored zero-phase-difference for step-scan), and the Blackman–Harris 3-term apodization function. Absorption noise is calculated as the rms value of difference spectra between 1700 and 1800 cm^{-1} , a region where there are no Stark effect signals.

For DC and synchronized AC spectra, the interferogram was sampled at every laser zero-crossing, yielding 29 324 interferogram points and spectra over the full 0 – $15\,798\text{ cm}^{-1}$ acquisition range. As shown below, this interferogram oversampling reduces the spectral noise. DC measurements used a 20 kHz mirror speed (the temporal frequency of the HeNe laser signal) and co-added 1206 scans (1206 field-on scans and 1206 field-off scans). AC measurements used a 5 kHz mirror speed and 286 scans. A 16 kHz low-pass electronic filter was used for the DC method, although comparison with other measurements shows that it did not help significantly.

For step-scan spectra, the acquisition range was reduced to 1216 – 2430 cm^{-1} , which is the smallest range possible with the interference filter used; this required 2225 interferogram points. A Stanford Research Systems SR850 lock-in amplifier was used for generation of the 2 kHz electric-field signal and for detector-signal demodulation (phase modulation was not used). The lock-in was configured to have a 100-ms time constant and 12 dB/octave roll-off on the output low-pass filter, which gave a 1.2 Hz noise equivalent bandwidth. Since a large transient detector signal is created at each mirror step, the lock-in was allowed to stabilize for 1 s after each step

before data collection, which was found to be the minimum stabilization time that yielded difference spectra without artifacts. (The mirror is effectively stationary after about 20 ms, so the vast majority of this time is used for signal averaging by the lock-in.)

Double modulation was attempted as well. In this case, a 1.6-kHz mirror speed was used, 212 scans, a 2-kHz electric field, and either a 100- μ s or a 300- μ s lock-in time constant. While signal-to-noise ratios were nearly as good as for other methods, results were inconsistent and disagreed with other results, leading us to believe that they were dominated by artifacts. Since we could not separate the frequencies further, double modulation was not pursued and is not discussed below.

For measurements of detector noise, the interference filter was removed and a black card was immersed in liquid nitrogen at the sample position. The card effectively blocked all incident light and, being cold, had little emission of its own.

RESULTS

Sources of Noise. Noise sources in FT-IR measurements include light source fluctuations, background light fluctuations, sample fluctuations, interferogram sampling at slightly unequal retardation intervals, amplifier noise, and bit noise on the analog-to-digital converter.²⁴ On most commercial FT-IRs, great care has been taken to reduce all the forms of noise as much as possible, leaving the sample and detector as the dominant sources. For the experiments presented here, sample fluctuations were examined by comparing interferogram noise between scans with and without the sample and cryostat in the beam-path. They were essentially the same, showing that sample fluctuations add a negligible contribution to the total noise. To examine bit noise, a pair of identical interferograms was measured with a single scan each. The difference showed noise with no digitization effects, indicating that bit noise is negligible as well.

For quantum-type infrared detectors, such as InSb and MCT detectors, noise is often dominated by statistical photon fluctuations of background infrared light. This light, which is simply the thermal radiation of anything within the detector's field of view, leads to white noise in the spectrum (the same amount of noise at all frequencies). If the background fluctuations are eliminated, the remaining sources of detector noise are noise due to the detector current,²⁵ which has a $1/f$ frequency dependence, and the Johnson noise of the detector,²⁶ which is white noise. We measured the frequency distribution of noise for our MCT detector with the detector facing a 77 K black card, as described above, over frequencies from 0.25 Hz to 80 kHz. This method excludes all sources of noise other than that from the detector and amplifiers. Noise was nearly constant up to 20 kHz and then decreased, reaching a factor of 3 decrease by 80 kHz. Using the same data, but in the time domain, the rms noise was 1.3×10^{-4} V.

DC Stark Spectroscopy. The measured detector voltage after the pre-amplifier has both a "noise-free" component, $V(\delta)$, which is proportional to the light intensity, and a noise component, $N(\delta)X$, where δ is the mirror retardation. $N(\delta)$ is the rms noise level and X is a random

variable with unit variance. The measured voltage comprises an interferogram,

$$V_{\text{meas.}}(\delta) = V(\delta) + N(\delta)X. \quad (1)$$

The Fourier transform of the interferogram, with appropriate apodization and phase correction, yields a single channel spectrum,²⁴

$$B_{\text{meas.}}(\bar{\nu}) = \frac{2}{n_{\text{pts}}} \sum_{j=1}^{n_{\text{pts}}} V_{\text{meas.}}(\delta_j) \exp(-2\pi i \delta_j \bar{\nu}) \quad (2)$$

$$= B(\bar{\nu}) + \sqrt{\frac{2}{n_{\text{pts}}}} N(f)X. \quad (3)$$

The factor of 2 in the Fourier transform arises from basic FT-IR signal analysis for a single sided interferogram. The f is the modulation frequency of wavenumber $\bar{\nu}$, called the Fourier frequency ($f = 2\nu\bar{\nu}$, where ν is the mirror velocity), and n_{pts} is the number of points in the interferogram. $B(\bar{\nu})$ can be understood as the "noise-free" detector voltage that would be observed if the interferometer were replaced with a perfect monochromator that just passed light between $\bar{\nu}$ and $\bar{\nu} + \Delta\bar{\nu}$, where $\Delta\bar{\nu}$ is the spectral resolution. $N(f)$ is the rms noise of the detector signal at frequency f . From the central limit theorem, the variance of the sum of n_{pts} uncorrelated random variables, each with unit variance, is n_{pts} . In the Fourier transform, half of the result is imaginary, leading to a variance of the real component of $n_{\text{pts}}/2$, a real rms value of $(2n_{\text{pts}})^{-1/2}$, and thence the final result given above. This analysis depends upon the assumptions that the noise is white noise and that it is additive rather than multiplicative; from the discussion above, these are valid for the dominant portion of the noise in these experiments.

In the case of Stark measurements using a DC field technique, the difference absorption is the negative log of the ratio of the field-on single channel spectrum and the field-off single channel spectrum. Including noise effects, the measured Stark absorption spectrum for a single pair of scans is

$$\Delta A_{\text{meas.}}(\bar{\nu}) = -\log \frac{B_{\text{on}}(\bar{\nu}) + \sqrt{\frac{2}{n_{\text{pts}}}} N_{\text{on}}(f)X}{B_{\text{off}}(\bar{\nu}) + \sqrt{\frac{2}{n_{\text{pts}}}} N_{\text{off}}(f)X} \quad (4)$$

Since the Stark effect yields a small absorption change, $B_{\text{on}}(\bar{\nu})$ is very similar to $B_{\text{off}}(\bar{\nu})$. Also, the noise voltages are much smaller than the signal voltages. These simplify Eq. 4 to

$$\Delta A_{\text{meas.}}(\bar{\nu}) = \Delta A(\bar{\nu}) - \frac{\sqrt{2} \Delta N(f)}{\ln(10) \sqrt{n_{\text{pts}}} B_{\text{off}}(\bar{\nu})} X, \quad (5)$$

where $\Delta A(\bar{\nu})$ is the "noise-free" Stark spectrum and $\Delta N(f)$ is $N_{\text{on}}(f) - N_{\text{off}}(f)$. $\Delta N(f)$ is a factor of $2^{1/2}$ larger than the noise in a single spectrum since it is the difference between a pair of uncorrelated noise values. If n_{sc} reference scans are averaged together and n_{sc} sample scans are averaged together, the average noise values de-

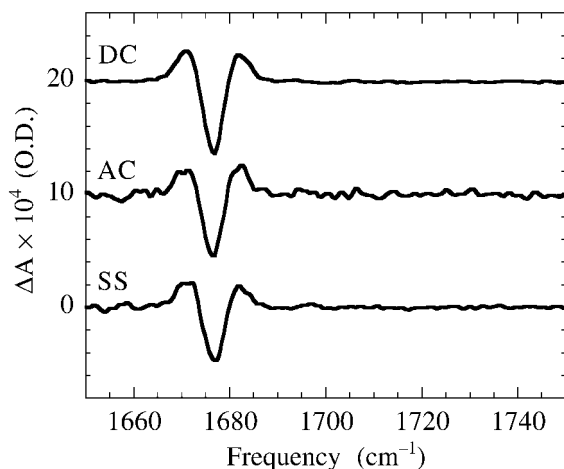


FIG. 2. Raw data for vibrational Stark spectra of methyl-vinyl-ketone measured with each method. Spectra for the DC method and synchronized AC method are offset for clarity. All spectra were measured at 77 K, with a 0.5 MV/cm peak field, 1 cm⁻¹ resolution, and with 40 min of signal averaging.

crease by a factor of $n_{sc}^{1/2}$, again due to the lack of noise correlations between different scans. These factors are included to give the final result for multiple co-added scans,

$$\Delta A_{\text{meas.}}(\bar{\nu}) = \Delta A(\bar{\nu}) - \frac{2N(f)}{\ln(10)\sqrt{n_{sc}n_{pts}B_{\text{off}}(\bar{\nu})}}X \quad (6)$$

This result does not depend on the order of field-on and field-off scans, which can be traced to the assumption of white noise. However, there is actually slightly more noise at very low frequencies than elsewhere, due to the detector current and detector drift. These factors were nearly eliminated by interleaving sample and reference scans.

Using just the experimental detector noise, along with the measurement parameters given above, the absorption noise is calculated for a 40 min measurement to be 3.6×10^{-6} o.d., in good agreement with the experimental noise (Fig. 2), 4.6×10^{-6} o.d. The close agreement shows that most of the noise in the measured Stark spectrum is from the detector.

Synchronized AC Spectroscopy. The synchronized AC method gets around the restriction that the frequencies be well separated by having the field synchronized to the sampling of the interferogram. However, the mirror still had to be slowed down to give the Stark cell time to fully charge or discharge between interferogram sampling points. Looking back to Eqs. 1 through 6, it can be seen that they also apply for synchronized AC measurements. The only differences are that f is now approximately twice the field frequency to account for the modulation and n_{sc} is reduced due to the slower mirror speed. The result is that the expected noise doubles, giving a value of 7.5×10^{-6} o.d. of noise in a 40 min measurement. The measured noise was somewhat larger, with a value of 12.6×10^{-6} o.d.

While the noise in synchronized AC measurements is consistently larger than that for DC measurements, the AC method is still useful. While developing Stark spectroscopy methods, we showed that sample molecules did

not become aligned with an external electric field on timescales longer than 1 s,¹ suggesting, but not proving, that the sample was fully immobilized. As the synchronized AC method yields results that are identical to previous ones, which used the DC method, it is now seen that there is negligible sample alignment on timescales as short as 0.4 ms, allowing increased confidence in the original data and in comparable data. A second benefit of the AC method is that it is less susceptible to low frequency noise. As a result, baselines are not offset from zero, as they sometimes are for DC measurements, and baselines are also significantly flatter. This is especially valuable for difference spectroscopy of very broad peaks, such as a mid-infrared electronic transition in the photosynthetic reaction center,²⁷ for which it would be useful to have Stark effect results.²⁸

Step-Scan Stark Spectroscopy. Using the same notation as before, a difference interferogram in the presence of noise for the step-scan method is

$$\Delta V_{\text{meas.}}(\delta) = \Delta V(\delta) + \Delta N(\delta)X \quad (7)$$

In this case, the noise term is the noise that passes through the lock-in amplifier. It can be estimated by using the measured rms noise for the MCT detector, 1.3×10^{-4} V, and the approximate frequency range over which white noise was observed, 20 kHz, to yield a detector noise density, e_n , of 9×10^{-7} V(Hz)^{-1/2}. The equivalent noise bandwidth of the lock-in, $\Delta f_{\text{lock-in}}$, was 1.2 Hz, yielding transmitted noise of 1×10^{-6} V. Fourier transforming, as in Eq. 3, yields the difference single channel spectrum,

$$\Delta B_{\text{meas.}}(\bar{\nu}) = \Delta B(\bar{\nu}) + \frac{1}{\sqrt{n_{pts}}}e_n\sqrt{\Delta f_{\text{lock-in}}}X \quad (8)$$

The noise term here is a factor of 2^{1/2} smaller than it was for the DC method because half the noise appears in the lock-in quadrature signal and so does not appear in the difference spectrum.

A reference intensity, $B_{\text{off}}(\bar{\nu})$, is measured separately in rapid-scan mode with the electric field turned off. Since $\Delta B_{\text{meas.}}(\bar{\nu})$ is much smaller than $B_{\text{off}}(\bar{\nu})$, the Stark absorption spectrum can be approximated as

$$\Delta A_{\text{meas.}}(\bar{\nu}) = -\frac{2\sqrt{2}\Delta B_{\text{meas.}}(\bar{\nu})}{\ln(10)B_{\text{off}}(\bar{\nu})}X \quad (9)$$

where the factor of $2\sqrt{2}$ accounts for the difference between rms and peak voltage and for the second harmonic of the field.¹⁴ Combining Eqs. 8 and 9 yields the final result

$$\Delta A_{\text{meas.}}(\bar{\nu}) = \Delta A(\bar{\nu}) - \frac{2\sqrt{2}e_n(f)\sqrt{\Delta f_{\text{lock-in}}}}{\ln(10)\sqrt{n_{pts}B_{\text{off}}(\bar{\nu})}}X \quad (10)$$

Using this equation and the assumptions above, the noise is calculated to be 3.5×10^{-6} o.d., which can be compared to 8.4×10^{-6} o.d. of experimental noise.

DISCUSSION

It is seen that the experimental noise was consistently larger than the calculated noise. A contributing factor for

all the methods is that the detector noise was measured with essentially no incident light and minimal detector current, whereas the Stark experiments involved a probe light and a significant detector current, thereby adding some noise. Also, Stark measurements included random background thermal emission from the interference filter. Step-scan experiments are subject to a variety of other noise sources as well, which were not included in the calculation. They are known to be very sensitive to instrument vibrations from building motion and acoustic noise, to low frequency multiplicative fluctuations such as source drift,²⁹ and to lock-in limitations, which can be reduced by replacing the lock-in amplifier with a digital signal processor.^{30,31}

Equations 6 and 10 have several dependencies in common, which can be used for understanding and minimizing experimental noise. Noise is inversely proportional to $B_{\text{off}}(\bar{\nu})$, implying that noise can be reduced by maximizing the light throughput at the frequency of interest. In practice, detector noise increases with increasing light, but as the noise does not increase as fast as the signal over most of the available intensity range, it is advantageous to use high light throughputs.[†] The noise is also inversely proportional to $n_{\text{pts}}^{1/2}$. This implies that for the DC and synchronized AC methods, oversampling of the interferogram is a simple way to reduce noise without taking any more scan time. On the other hand, each interferogram point takes a fixed amount of time in the step-scan method, so in that case, one wants to sample the fewest points possible by using a narrow optical bandpass filter. Thus, the DC and synchronized AC methods are best for broad spectral ranges whereas step-scan is best for narrow spectral ranges. Doubling the resolution (halving $\Delta\bar{\nu}$) while maintaining a constant measurement time affects several factors: n_{pts} is doubled, n_{sc} is halved, $\Delta f_{\text{lock-in}}$ is doubled, and $B(\bar{\nu})$ is halved. Thus, for all the methods, doubling the resolution doubles the rms noise. However, when the data are analyzed, this yields twice as many data points in a spectral region, so fit errors only increase by a factor of $2^{1/2}$.

In DC and synchronized AC methods, low noise is achieved by averaging many data points over many scans. They also make use of the multiplexing advantage, in which all frequencies incident on the detector are collected and used. The step-scan method, by contrast, uses relatively few data points, does not make use of signal multiplexing, and spends a large fraction of the total scan time waiting for the lock-in to settle. However, the excellent noise rejection of the lock-in amplifier (which is a direct consequence of the long settling time and the lack of multiplexing) makes up for the other factors, yielding very similar noise results in the end for the parameters used here.

The data presented here show that our original method

of measuring vibrational Stark spectra on an FT-IR, using a DC field, performs better than either synchronized AC or step-scan methods. However, the differences in signal-to-noise values are small, so specific situations may favor the other methods. In particular, the synchronized AC method can be used over a large spectral range but still yields very flat baselines while the step-scan method should perform the best for narrow spectral ranges. It is possible to predict quantitative noise levels for any of the three experimental methods from Eqs. 6 and 10, which are seen to approximate measured values moderately well.

ACKNOWLEDGMENTS

We thank Eunice Park for the methyl-vinyl-ketone sample and Joe Rolfe for helping to design and build the field controller. This work was supported in part by grants from the NSF Chemistry Division and the NIH. The FT-IR facilities are supported by the Medical Free Electron Laser Program of the Office of Naval Research under Contract N00014-94-1-1024.

1. S. S. Andrews and S. G. Boxer, *J. Phys. Chem. A* **104**, 11853 (2000).
2. E. S. Park, S. S. Andrews, R. B. Hu, and S. G. Boxer, *J. Phys. Chem. B* **103**, 9813 (1999).
3. N. S. Hush and J. R. Reimers, *J. Phys. Chem.* **99**, 15798 (1995).
4. S. S. Andrews and S. G. Boxer, *J. Phys. Chem. A*, in press (2001).
5. V. Abetz, G. G. Fuller, and R. Stadler, *Polym. Bull.* **23**, 447 (1990).
6. L. A. Nafie, *Appl. Spectrosc.* **50**, 14A (1996).
7. M. J. Green, B. J. Barner, and R. M. Corn, *Rev. Sci. Instrum.* **62**, 1426 (1991).
8. B. O. Budevaska and P. R. Griffiths, *Anal. Chem.* **65**, 2963 (1993).
9. C. Korzeniewski, *Crit. Rev. Anal. Chem.* **27**, 81 (1997).
10. X. Hu, H. Frei, and T. G. Spiro, *Biochemistry* **35**, 13001 (1996).
11. I. Noda, A. E. Dowrey, C. Marcott, G. M. Story, and Y. Ozaki, *Appl. Spectrosc.* **54**, 236A (2000).
12. S. E. Plunkett, J. L. Chao, T. J. Tague, and R. A. Palmer, *Appl. Spectrosc.* **49**, 702 (1995).
13. S. V. Shilov, S. Okretic, H. W. Siesler, and M. A. Czarnecki, *Appl. Spectrosc. Rev.* **31**, 125 (1996).
14. G. U. Bublitz and S. G. Boxer, *Annu. Rev. Phys. Chem.* **48**, 213 (1997).
15. R. A. Palmer, J. L. Chao, R. M. Dittmar, V. G. Gregoriou, and S. E. Plunkett, *Appl. Spectrosc.* **47**, 1297 (1993).
16. F. Long, T. B. Freedman, T. J. Tague, and L. A. Nafie, *Appl. Spectrosc.* **51**, 508 (1997).
17. E. D. Lipp, C. G. Zimba, and L. A. Nafie, *Chem. Phys. Lett.* **90**, 1 (1982).
18. E. D. Lipp and L. A. Nafie, *Appl. Spectrosc.* **38**, 20 (1984).
19. F. Long, T. B. Freedman, R. Hapanowicz, and L. A. Nafie, *Appl. Spectrosc.* **51**, 504 (1997).
20. P. A. Berg and J. J. Sloan, *Rev. Sci. Instrum.* **64**, 2508 (1993).
21. J. Lindner, J. K. Lundberg, R. M. Williams, and S. R. Leone, *Rev. Sci. Instrum.* **66**, 2812 (1995).
22. K. Masutani, H. Sugisawa, A. Yokota, Y. Furukawa, and M. Tasumi, *Appl. Spectrosc.* **46**, 560 (1992).
23. K. Masutani, K. Numahata, K. Nishimura, S. Ochiai, Y. Nagasaki, N. Katayama, and Y. Ozaki, *Appl. Spectrosc.* **53**, 588 (1999).
24. P. R. Griffiths and J. A. de Haseth, *Fourier Transform Infrared Spectrometry* (John Wiley and Sons, New York, 1986).
25. A. L. Vinson and E. L. Dereniak, *Proc. SPIE-Int. Soc. Opt. Eng.* **572**, 109 (1985).
26. D. N. B. Hall, R. S. Aikens, R. Joyce, and T. W. McCurnin, *Appl. Opt.* **14**, 450 (1975).
27. J. Breton, E. Nabedryk, and W. W. Parson, *Biochemistry* **31**, 7503 (1992).
28. J. R. Reimers, M. C. Hutter, and N. S. Hush, *Photosynth. Res.* **55**, 163 (1998).
29. C. J. Manning and P. R. Griffiths, *Appl. Spectrosc.* **51**, 1092 (1997).
30. C. J. Manning and P. R. Griffiths, *Appl. Spectrosc.* **47**, 1345 (1993).
31. D. L. Drapcho, R. Curbelo, E. Y. Jiang, R. A. Crocombe, and W. J. McCarthy, *Appl. Spectrosc.* **51**, 453 (1997).

[†] A cooled interference filter, which passes just the spectral region of interest, can be placed over the detector element to block unnecessary light and reduce detector noise. It also does not emit much light since it is cooled, and it moves the interferogram intensity away from the centerburst and into the wings, which allows the use of a brighter light source, larger aperture, and greater amplification of the detector signal.